Applied Chemical Engineering (2023) Volume6 Issue 2
doi: 10.24294/ace.v6i2.2073

ORIGINAL RESEARCH ARTICLE

Preparation and characterization of ATP-loaded chitosan/alginate nanoparticles for therapeutic applications

Gopikrishna Agraharam, Agnishwar Girigoswami, Koyeli Girigoswami*

Faculty of Allied Health Sciences, Chettinad Hospital and Research Institute, Chettinad Academy of Research and Education, Chettinad Health City, Chennai 603103, India

*** Corresponding author:** Koyeli Girigoswami, koyelig@gmail.com

ABSTRACT

Adenosine triphosphate (ATP) is known as an energy source and is generated by mitochondria which is the powerhouse of the cell. The ATP supplies energy through the disassociation of the phosphate group by the cellular enzymes. The extracellular ATP in the extracellular environment acts as a signaling molecule and can act as an anti-inflammatory molecule, can promote cancer progression, and also can act as a pro-inflammatory molecule. The degradation of ATP is a major disadvantage by ectonucleotidases that attenuates the therapeutic property of ATP in the extracellular environment. We have formulated chitosan/alginate nanoparticles loaded with ATP for increasing their encapsulation efficiency and for sustained drug release. This encapsulation can avoid ATP degradation from ectonucleotidases. Nanoparticle characterization by DLS, FTIR, SEM, encapsulation efficiency, and cytotoxicity assay by XTT assay and Live-dead assay was monitored for the synthesized nano formulated ATP. Our results showed that the formulated ATP-loaded chitosan/alginate nanoparticle sized about 342 nm with the optimum encapsulation efficiency of about 92.03% with a sustained drug release profile. These nano formulated ATP could be used for calorie restriction conditions where ATP can be supplied as an extracellular source for bypassing oxidative phosphorylation, and we can circumvent the oxidant production during oxidative phosphorylation. The concept of avoiding oxidative stress by bypassing oxidative phosphorylation can open an avenue for healthy aging.

Keywords: chitosan; alginate; nanoparticles; ATP; ATP-loaded nanoparticles

ARTICLE INFO

Received: 28 April 2023
Accepted: 21 June 2023
Available online: 1 August 2023

1. Introduction

Adenosine triphosphate (ATP) is known as a cellular energy source that is produced in the process of electron transport chain (ETC), stored in the cell, and supplied to the cellular requirements. Intracellular ATP acts as an energy source for the cell whereas extracellular ATP (eATP) acts as a signaling molecule[1]. The eATP gets released from the cell into the extracellular space in response to different stimuli such as shear stress, ionizing/non-ionizing radiations, osmotic swelling, pH, stretch, inflammation, hypoxia, reactive oxygen species, cell death signals, and purine 2 (P2) receptors. The P2 is classified as ionotropic P2X receptors and metabotropic P2Y receptors. The eATP and its metabolites such as ADP, and AMP bind with these P2X, P2Y/P1 receptors and contribute to various physiological functions. The ATP concentrations range from 1 μM, 10–100 μM, and 0.5–1.0 mM[2,3], and can activate P2Y, P2X, and P2X7 receptors respectively[4]. In the tumor microenvironment (TME) it can promote tumor and can also suppress tumor progression depending on ATP concentration which indicates the vital role of

ATP in targeting cancer[5]. In the TME, ectonucleotidases such as CD39 (ecto-nucleoside triphosphate diphosphohydrolase) and CD73 (ecto-5'-nucleotidase) hydrolyzes ATP to ADP (Adenosine diphosphate), AMP (Adenosine monophosphate), and AMP to adenosine, respectively. Inflammation promotes the accumulation of ATP which acts as a key danger signal and triggers pro-inflammatory responses. Sequential degradation happens from ATP to ADP, AMP, and AMP to adenosine by CD39 and CD73, and the converted adenosine promotes a depressive action on the immune cell activity and shows a potent anti-inflammatory effect[6]. The eATP can cause cell plasma membrane permeability changes and severely affects intracellular ion balance which can lead to ATP-dependent cytotoxicity due to increased ATP concentration[7,8]. Reports published previously indicated that intraperitoneal injection of ATP (50 mM) into the tumor-possessing mice was found to show reduced tumor size. eATP treatment was found to inhibit the growth of cancer cells by arresting the cell cycle at the S phase[9,10]. Studies on in vivo human prostate cancer xenografts with eATP intraperitoneal administration daily showed tumor regression[11].

A rapid degradation of eATP by ectonucleotidases is a disadvantage of ATP activity and thus requires a system for the sustained release of eATP at the required sites for its efficient activity and protection from the degradation by the ectonucleotidases. Du et al. formulated ATP-loaded chitosan oligosaccharide nanoparticles by using various concentrations of chitosan oligosaccharides and reported encapsulation efficiency of 40.6%–69.5% and ATP loading of 3.9%–6.5%[12]. Konno et al. reported liposomes entrapped with ATP and found 8% of ATP entrapment efficiency[13].

Nanotechnology is been explored in recent times for its versatile applications in nano enabled drug delivery[14], imaging and theranostics[15–17], improving the bioavailability of phytochemicals[18,19], biosensing[20], photoremediation[21–24] as well as photodynamic therapy[25]. Using chitosan coated with sodium alginate nanoparticles offers a versatile platform for delivering small molecules like ATP, drugs, etc., providing improved stability, solubility, controlled release, high loading efficiency, and protection from hostile physiological conditions. These advantages make them promising candidates for various biomedical and pharmaceutical applications. In this study, to attenuate ectonucleotidases' metabolism of ATP and to increase encapsulation efficiency and sustained release of ATP, we have formulated ATP-loaded chitosan (CS)/alginate (Alg) nanoparticle that showed a sustained release of ATP and encapsulation efficiency of about 92.03%. The characterization of the nano formulated ATP was executed using different photophysical tools such as dynamic light scattering, scanning electron microscopy, and FTIR. To assess the biocompatibility of this nanoformulation, cell viability using normal cell line L132 was also assessed.

2. Materials

Chitosan, Alginate are procured from HiMedia, India. Acridine orange, Dulbecco's modified eagle medium (DMEM), Fetal bovine serum (FBS) (Gibco, USA), Antibiotic solution (Antibiotic Solution 100X Liquid w/ 10,000U Penicillin and 10 mg Streptomycin per ml in citrate buffer), XTT reagent, ATP purchased from SRL, India. L132 (embryonic lung cells) was procured from NCCS, Pune. Ethidium bromide, and acridine orange were procured from Sigma Aldrich.

3. Methodology

3.1. Nanoformulation of ATP-loaded chitosan/alginate Nanoparticle

To the 10 mL of sodium alginate solution (3 mg/mL, pH 5.1), we added 2 mL of calcium chloride ($CaCl_2$) solution (3.35 mg/mL) dropwise while it was on continuous stirring for 20 min. Later, to this, we added ATP in three different concentrations to three sodium alginate solutions (50 mg, 75 mg, and 100 mg) and allowed 30 min stirring. After that 4 mL of chitosan (800 µg/mL in 1% acetic acid, pH 5.4) was added to this solution and left for 30 min stirring and was allowed for overnight incubation at room temperature. Later, the solution was used to take drug absorbance (OD at 260 nm) to measure the total drug OD, for

encapsulation efficiency, and then the solution was centrifuged at 3000 rpm (454 RCF) for 15 min and the supernatant was collected to measure the unbound drug OD. To the ATP-loaded alginate/ chitosan (ATP-CS/Alg) pellet, distilled water was added and centrifuged in order to wash it and discarded the supernatant. Further, it was gently mixed by adding 5 mL of distilled water and it was stored at 4 °C for further use[26].

3.2. Characterization

The size of the nanoparticle and its zeta potential was analyzed by using the Malvern zeta sizer instrument. The functional group confirmation was done by using an FTIR instrument, surface scanning was performed using JEOL JEM 2100 HRTEM with an accelerating voltage of 200 kV.

3.3. Encapsulation efficiency

The % of encapsulation efficiency (EE) was calculated as per the given formula[27].

$$\%\ of\ Encapsulation\ Efficiency = \frac{Total\ drug\ OD - Unbound\ Drug\ OD}{Total\ Drug\ OD} \times 100$$

3.4. Cumulative drug release kinetics

The cumulative drug release kinetics of ATP-loaded CS/Alg NPs was analyzed using a dialysis membrane (2 KDa cutoff) in a phosphate buffer saline (PBS) (1X (10 mM), pH 7.4) at room temperature. We found the optimum encapsulation efficiency for the 75 mg loaded CS/Alg NPs from our experiments on encapsulation efficiency, so we conducted further studies using 75 mg loaded CS/Alg NPs and named it nATP. We loaded 2 mL of 75 mg loaded CS/Alg NPs (nATP) in the dialysis membrane and dipped the membrane in 25 mL of PBS with continuous stirring using a magnetic bead. At specific time intervals, 2 mL of the buffer was withdrawn and the same volume of PBS was replenished for maintaining the total volume, and the absorbance was measured for the aspirated solution. The amount of released ATP from the nanoparticle was spectrophotometrically measured by taking absorbance at 260 nm at different time intervals[26].

3.5. XTT assay

The cell viability assay was measured using XTT assay using L132 cells after treatment with only ATP and nanoformulated ATP (nATP) as done previously[28]. The L132 cells (2×10^4 cells/well) were seeded in equal numbers in a 96-well plate and supplemented with DMEM containing 10% FBS, and 1% antibiotic solution, maintained in a humidified atmosphere at 37 °C and 5% CO_2. After 24 h the cells were treated with various concentrations of ATP and ATP-loaded CS/Alg NPs (2–8 mM). After 24 h of incubation, the cells were treated with 50 µL activated XTT reagent and then allowed for 4 h of incubation at 37 °C and 5% CO_2, in a humidified atmosphere. Then, the absorbance was taken at 450 nm.

3.6. Live-dead assay

Coverslips were dipped in 70% ethanol, air dried, and then placed on 35 mm cell culture dishes containing 2 mL of DMEM medium (10% FBS, 1% antibiotic solution) and L132 cells were added to the plate. When the cells reached 70% confluency, they were treated with ATP-loaded CS/Alg NPs, and the control was kept untreated. After 24 h of treatment, the DMEM from the culture plate was removed and we added 1 mL of dye solution. The dye solution was immediately prepared in the dark by adding 5 µL acridine orange (1.2 mM) and 2 µL ethidium bromide (1.9 mM) and was made up to 2 mL with PBS. The concentration of the staining solution was standardized in our previous studies[29]. After adding the stain to the cells under dark conditions, the cells were incubated for 3 min at 37 °C. Later the cover slip that contained the cells was taken out with forceps and placed on a glass slide and observed under a fluorescence microscope (Olympus BX51 Fluorescence Microscope). The live cells (appeared in green color) and the dead cells (appeared in red) were monitored and counted at 5 different places throughout the coverslip. The

percentage of dead cells was calculated using the formula given below[29].

$$\%\ of\ dead\ cells = \frac{Total\ number\ of\ dead\ cells}{Total\ number\ of\ cells} \times 100$$

4. Results and discussion

4.1. Characterization

Size and zeta potential of nanoparticles

The size of the nanoparticle and its zeta potential was analyzed by using the Malvern zeta sizer instrument. The hydrodynamic diameter of CS/Alg NPs and 50 mg, 75 mg and 100 mg ATP-loaded CS/Alg nanoparticles were found to be 43 nm, 144 nm, 342 nm, and 825 nm, respectively (**Figure 1a**). The zeta potentials measured for only CS/Alg and the 50 mg, 75 mg, and 100 mg ATP-loaded CS/Alg nanoparticles are given in **Table 1**. The hydrodynamic diameter was lower for only CS/Alg mixed polymer which increased with an increase in the amount of ATP added. The increase in hydrodynamic diameter shows that the ATP has been incorporated into the mixed polymer matrix. The zeta potential values indicated that the mixed polymer was highly stable (−31 mV). After ATP encapsulation also the structures were highly stable as indicated by the zeta potential values. Among the ATP loading, 100 mg ATP exhibited a higher hydrodynamic diameter whereas 50mg and 75 mg ATP-loaded nanoformulation showed lower hydrodynamic diameter which is suitable for nano-enabled drug delivery. Moreover, both 50 mg and 75 mg had similar stability. For our studies, we used 75 mg ATP-loaded CS/Alg mixed polymer (nATP) which had a hydrodynamic diameter of 342 nm and zeta potential of −10 mV.

Table 1. Size and zeta potential of nanoparticles.

S/ No.	Sample name	Zeta potential (mV)
1.	CS-Alg NPs	−31.0
2.	50 mg ATP-loaded CS-Alg NPs	−9.6
3.	75 mg ATP loaded CS-Alg NPs	−10.0
4.	100 mg ATP loaded CS-Alg NPs	−21.0

4.2. Functional group confirmation by FTIR

4.2.1. Chitosan FTIR analysis

Nanoparticle formation was confirmed by FTIR spectroscopy, and the peaks at wavenumber 3449 cm^{-1} corresponded to $–NH_2$ and –OH stretching and also indicated intramolecular hydrogen bonds. The peak at 2920 cm^{-1} was derived from the symmetric and asymmetric C–H bond stretching of the polysaccharide. Wavenumber at 1640 cm^{-1} (C = O stretching of amide I) and 1323 cm^{-1} (C–N stretching of amide III) corresponded to amide I and amide III stretching, respectively; whereas the peak at 1557 cm^{-1} corresponded to the N–H bending of amide II. The bands at 1416 and 1377 cm^{-1} indicated CH_2 bending and CH_3 symmetrical deformations. The band at 1153 cm^{-1} corresponded to the symmetric stretching of the C–O–C bridge. 1073 cm^{-1} confirmed the C–O stretching of chitosan. The bands found from the chitosan sample FTIR spectra showed similar peaks to previously reported data[30–33] (**Figure 1b**).

4.2.2. Sodium alginate FTIR analysis

The peak at 3638 cm^{-1}confirmed the presence of –OH stretch, the absorption band at 1605 cm^{-1} corresponded to the carboxylate anions' intense stretching vibrations/asymmetric stretching vibration of COO– groups, 1412 cm^{-1} corresponded to the symmetric stretching vibrations of COO– groups, and the absorption band at 1028 cm^{-1} indicated elongation of C–O groups. The identified FTIR bands of sodium alginate was found to be similar to the previously reported results[34–36] (**Figure 1b**).

4.2.3. Chitosan/Alginate nanoparticle

The formulated Chitosan (CS)/Alginate (Alg) nanoparticle sample FTIR data was collected and the broad peak in the range of 3452 cm^{-1} corresponded to the –OH stretching, polymeric associations and also indicated CS and Alg intermolecular hydrogen bonds binary blend. Peaks at wavenumber 2934 cm^{-1} and 2356 cm^{-1} indicated asymmetric –CH stretching and symmetric –CH stretching. Peaks at 1634 cm^{-1}, 1416 cm^{-1} corresponded to the carbonyl group and NH bending (amide II band), respectively. The FTIR spectra indicated that COO– group was dissociated from a carboxylated group of alginate that was complexed with the amino group of chitosan through electrostatic interaction[37] (**Figure 1b**).

4.2.4. ATP and ATP-loaded CS/Alg nanoparticles

3439 cm^{-1} corresponded to the –OH stretching vibrations of ATP. The –OH/–NH_2 stretching vibrations of ATP-CS/Alg nanoparticles at wavenumber 3452 cm^{-1} were found to be shifted to lower wavenumber 3445 cm^{-1} after the loading/incorporation of ATP. The peak at 1634 cm^{-1} that corresponded to the amide group in the ATP-CS/Alg nanoparticle was found to be shifted to lower wavenumber 1630 cm^{-1} indicating the –OH group of ATP participation in the cross-linking reaction with CS/Alg nanoparticle. The asymmetric stretching vibration of the PO_2^- was found at 1260 cm^{-1} with a high absorbance in ATP, which was shifted to 1278 cm^{-1} for ATP-CS/Alg with a low intensity. The out-of-phase symmetrical stretches were found for both ATP and ATP-CS/Alg nanoparticles at 1066 cm^{-1} and 1079 cm^{-1}, respectively. Although, the transmittance was lower indicating that the ATP after incorporation into the CS/Alg nanoparticles, got restricted molecular movements. The P–O stretch of the main chain was observed for both ATP and ATP-CS/Alg nanoparticles at 918 cm^{-1} and 929 cm^{-1}, with high absorbance peak intensity for only ATP. These findings indicated that the ATP was incorporated inside the CS/Alg mixed polymer[38] (**Figure 1b**).

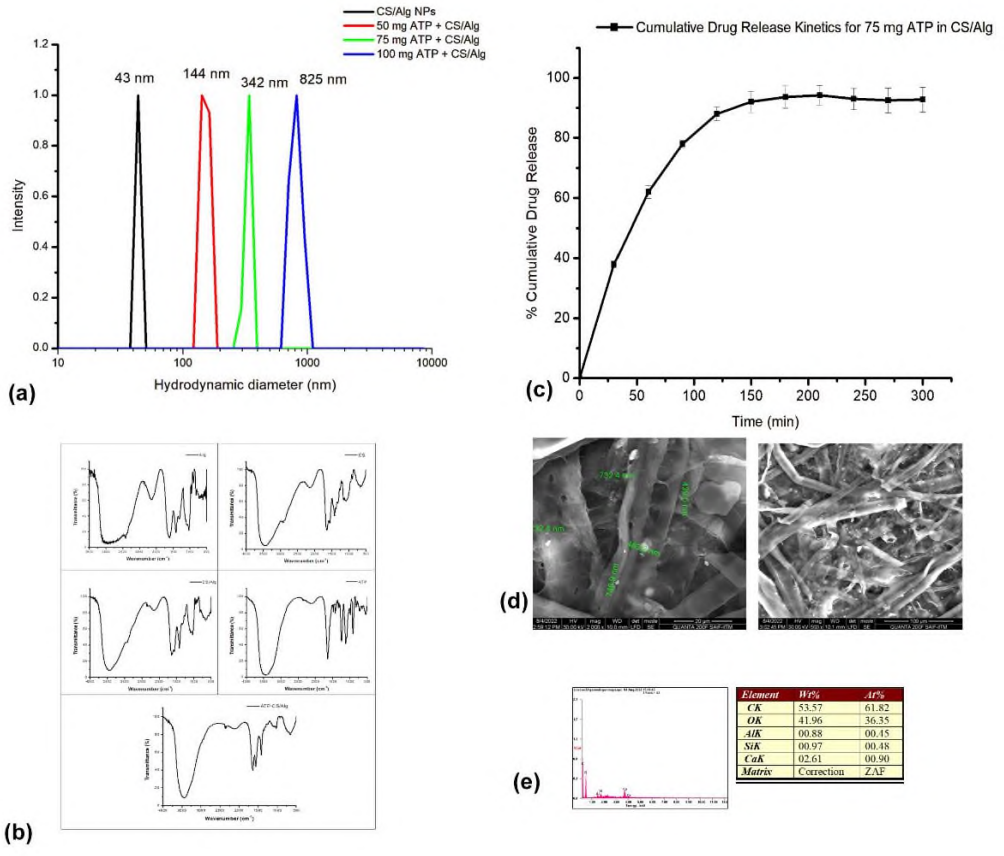

Figure 1. (a) The hydrodynamic diameter of CS/Alg Nanoparticles and ATP loaded CS/Alg Nanoparticles; **(b)** FTIR spectrum of Alg, CS, CS/Alg, ATP and ATP-CS/Alg; **(c)** Cumulative drug release kinetics graph; **(d)** SEM image of ATP loaded CS/Alg nanoparticle; **(e)** EDAX analysis of ATP loaded CS/Alg nanoparticle.

4.2.5. Encapsulation efficiency

The encapsulation efficiency for 50 mg, 75 mg, and 100 mg ATP-loaded CS/Alg NPs was found to be 73%, 92.03%, and 77.61%, respectively. The optimum encapsulation efficiency was found for the 75 mg ATP-loaded CS/Alg nanoparticle to be 92.03%. Earlier reports have found lower encapsulation efficiency of ATP when encapsulated in other polymeric matrices. ATP-loaded chitosan oligosaccharide nanoparticles exhibited 40.6%–69.5% encapsulation efficiency and ATP-loaded liposomes showed 8% entrapment efficiency[12,13]. Our ATP-loaded CS/Alg nanoparticle showed increased encapsulation efficiency which could be due to the chitosan and alginate cross-linkage, and so we proceeded the further experiments with 75 mg ATP-loaded CS/Alg NPs known as nATP.

4.2.6. Cumulative drug release kinetics

Cumulative drug release kinetics was done by using a dialysis membrane by taking 75 mg ATP-loaded CS/Alg nanoparticle against PBS (pH 7.4). The results showed sustained release of ATP. Almost 96 % of ATP was shown to be released after 5 h (**Figure 1c**). The release pattern followed zero-order kinetics which is desirable for the nanoformulated drugs for sustained release characteristics.

4.2.7. Scanning electron microscopy

The surface morphology of 75 mg ATP-loaded CS/Alg nanoparticle was shown in **Figure 1d**. The cross-linking of the CS/Alg mixed polymer shape was seen as a mesh structure that was sized at about 400–700 nm. A meshy structure of mixed polymer enabled them to encapsulate the lead molecule, ATP. A similar structure of the chitosan alginate copolymer was observed by previous researchers[39] where they have used the microfluidic spinning method to prepare the polymeric matrix. The EDX analysis also showed the presence of elements (C, O Si, Al, Ca) that are present in alginate and chitosan (**Figure 1e**). This indicated a successful synthesis of the mixed polymer.

4.2.8. Cytotoxicity assay

Cell viability assay was done using L132 cells by treating the cells with various concentrations (2, 4, 6, 8 mM) of ATP and ATP-loaded CS/Alg nanoparticles using XTT assay. ATP concentrations of more than 4 mM decreased the cell viability by about 30 % (**Figure 2a**). Our results showed that ATP-loaded CS/Alg nanoparticles showed higher cell viability than only ATP-treated cells indicating less cytotoxicity of ATP-loaded CS/Alg nanoparticles at every dose of treatment. Previous researchers have reported similar cytotoxic assay results of cervical cancer cells after ATP treatment and found that as the concentration of ATP increased the percentage of cell viability decreased[40]. Li et al. studied ATP cytotoxicity and found similar results and reported that ATP activated cell surface receptors at nanomolar/micromolar concentrations, and interfered with intracellular nucleotide pools at millimolar concentrations[41].

4.2.9. Live-dead assay

Live-dead assay was done by using acridine orange and ethidium bromide dyes. The results of ATP (4 mM) (**Figure 2b**) and ATP loaded CS/Alg nanoparticle (4 mM) (**Figure 2c**) treated cells were observed under a fluorescence microscope. The percentage of cell death was found to be 4.99% in ATP-treated cells and 1.19% in ATP-loaded CS/Alg nanoparticle treated cells. These results indicated that ATP-loaded CS/Alg nanoparticles were less toxic compared to only ATP.

ATP is the vital energy source in organisms and is generated within the cell through the mitochondria which is the powerhouse of the cell and is utilized for various cellular applications by supplying energy by dissociation of its phosphate group. ATP can be released into the extracellular space through various pathways which are considered eATP and can act as an extracellular signaling molecule.

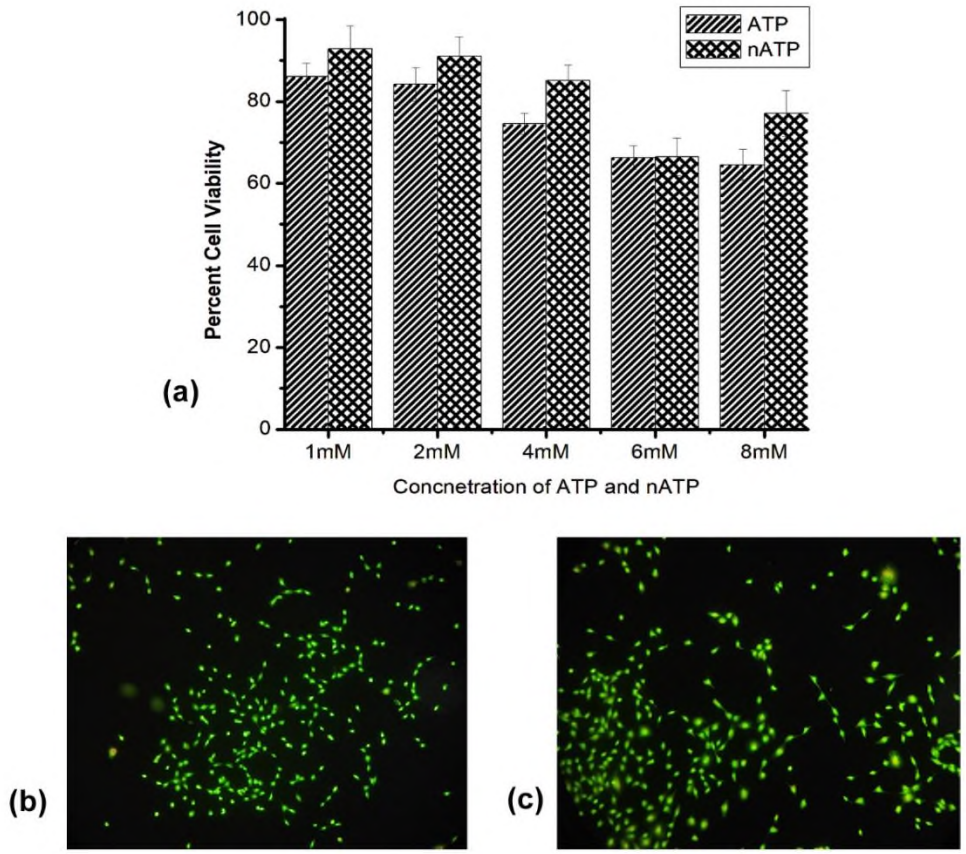

Figure 2. (a) Percentage of cell viability 24 h after treatment with different concentrations of ATP and nATP; **(b)** Live-dead assay for ATP treated L132 cells; **(c)** Live-dead assay for nATP (4 mM) treated L132 cells.

Here, we have formulated ATP loaded CS/Alg nanoparticle by the addition of 75 mg ATP that is sized about 342 nm and had a zeta potential of −10 mV with the optimum encapsulation efficiency of 92.03%. The drug release profile indicated the sustained release of ATP from ATP-loaded CS/Alg nanoparticles. Results from cell viability assay and live-dead assay showed that the formulated ATP-loaded CS/Alg nanoparticle was less toxic than only ATP.

A variety of physiological and pathophysiological circumstances cause cells to release ATP, which acts as an extracellular signaling molecule. There are several ectoenzymes involved in the metabolism of extracellular ATP and adenosine that determine their concentrations at their respective receptors[42]. An ectonucleotidase is an enzyme that metabolizes nucleotides externally oriented and expressed on the plasma membrane. A nucleoside is formed from nucleotides by these enzymes. Depending on the availability and preference of substrates, as well as the distribution of cells and tissues, ectonucleotidases modulate purinergic signaling[43]. Various types of cells produce ectonucleotidases that salvage purines and replenish ATP stores. As a result of dephosphorylation, nucleoside derivatives are absorbed into cells by membrane transporters. The enzyme ectonucleotidases modulates purinergic signaling at the P2 receptor, and at the P1 receptor as well[44]. Adenosine is also generated by ectonucleotidases; this causes adenosine receptors in the body to become activated, having opposite (patho-)physiological effects to nucleotides[45]. To avoid the action of the ectoendonucleases on ATP, we have nanoformulated the ATP in a mixed polymer. These results indicated that our ATP-loaded CS/Alg nanoparticle is less toxic and can be used for various applications in vitro studies and in vivo studies for assessing its prominent property as an extracellular energy molecule as well as a signaling molecule for releasing at a specific site.

5. Conclusion

In the present study, to increase the encapsulation efficiency, for the sustained release of ATP and to provide protection from the ectonucleotidases, we have prepared ATP-loaded CS/Alg nanoparticles. The presented characterization results and assay results of ATP and ATP-loaded CS/Alg nanoparticle treatment indicated that our formulated 75 mg ATP-loaded CS/Alg nanoparticle sized about 335.7 nm and zeta potential −10 mV with the encapsulation efficiency of about 92.03%. The drug release profile showed a sustained release of ATP. Cell viability assay and live-dead assay results proved ATP-loaded CS/Alg nanoparticles are less toxic than ATP to the L132 (embryonic lung cells). Thus, our results indicated that the formulated nanoparticle could be used for in vitro and in vivo research. In the process of aging, calorie intake plays a major role. If we can restrict the calories and can supplement the cells with extracellular ATP which is resistant to degradation by ectonucleotidases, it can reach the cells to produce energy. In this case, our formulated nano-ATP is a good alternative because it not only protects the ATP from degradation but also is highly stable in an aqueous environment. However, to demonstrate the ATP-loaded CS/Alg nanoparticle as a signaling molecule or as an energy source for therapeutic use further research is warranted.

Acknowledgments

The authors are grateful to the Chettinad Academy of Research and Education for supporting with CARE SEED Grant (Ref No. 004/Regr./AR-Research/2022-06).

Author contributions

Conceptualization, GA and KG; methodology, GA and KG; validation, KG and AG; formal analysis, KG and AG; investigation, GA and KG; data curation, GA; writing—original draft preparation, GA; writing—review and editing, GA, KG and AG; visualization, KG; supervision, KG; project administration, KG; funding acquisition, KG.

Funding

This research was funded by Chettinad Academy of Research and Education grant number 004/Regr./AR-Research/2022-06 .

Conflict of interest

The authors declare no conflict of interest.

References

1. Agraharam G, Girigoswami A, Girigoswami K. Calorie restriction and extracellular ATP on health and longevity—A perspective. *Current Nutrition & Food Science* 2023; 19(1): 4–8. doi: 10.2174/1573401318666220531111219
2. Lombardi M, Gabrielli M, Adinolfi E, Verderio C. Role of ATP in extracellular vesicle biogenesis and dynamics. *Frontiers in Pharmacology* 2021; 12: 654023. doi: 10.3389/fphar.2021.654023
3. Trautmann A. Extracellular ATP in the immune system: More than just a “danger signal”. *Science Signaling* 2009; 2(56): pe6. doi: 10.1126/scisignal.256pe6
4. Kojima S, Ohshima Y, Nakatsukasa H, Tsukimoto M. Role of ATP as a key signaling molecule mediating radiation-induced biological effects. *Dose-Response* 2017; 15(1): 1559325817690638. doi: 10.1177/1559325817690638
5. Vultaggio-Poma V, Sarti AC, Di Virgilio F. Extracellular ATP: A feasible target for cancer therapy. *Cells* 2020; 9(11): 2496. doi: 10.3390/cells9112496
6. Antonioli L, Pacher P, Vizi ES, Hasko G. CD39 and CD73 in immunity and inflammation. *Trends in Molecular Medicine* 2013; 19(6): 355–367. doi: 10.1016/j.molmed.2013.03.005
7. Rozengurt E, Heppel LA. A specific effect of external ATP on the permeability of transformed 3T3 cells. *Biochemical and Biophysical Research Communications* 1975; 67(4): 1581–1588. doi: 10.1016/0006-291x(75)90207-7

8. Landry Y, Lehninger AL. Transport of calcium ions by Ehrlich ascites-tumour cells. *Biochemical Journal* 1976; 158(2): 427–438. doi: 10.1042/bj1580427
9. Rapaport E. Treatment of human tumor cells with ADP or ATP yields arrest of growth in the S phase of the cell cycle. *Journal of Cellular Physiology* 1983; 114(3): 279–283. doi: 10.1002/jcp.1041140305
10. Rapaport E. Experimental cancer therapy in mice by adenine nucleotides. *European Journal of Cancer and Clinical Oncology* 1988; 24(9): 1491–1497. doi: 10.1016/0277-5379(88)90340-9
11. Shabbir M, Thompson C, Jarmulowiczc M, et al. Effect of extracellular ATP on the growth of hormone-refractory prostate cancer in vivo. *BJU International* 2008; 102(1): 108–112. doi: 10.1111/j.1464-410X.2008.07578.x
12. Du YZ, Ying XY, Wang L, et al. Sustained release of ATP encapsulated in chitosan oligosaccharide nanoparticles. *International Journal of Pharmaceutics* 2010; 392(1–2): 164–169. doi: 10.1016/j.ijpharm.2010.03.050
13. Konno H, Matin AF, Maruo Y, et al. Liposomal ATP protects the liver from injury during shock. *European Surgical Research* 1996; 28(2): 140–145. doi: 10.1159/000129451
14. Girigoswami K, Pallavi P, Girigoswami A. Targeting cancer stem cells by nanoenabled drug delivery. In: Pathak S, Banerjee A (editors).*Cancer Stem Cells: New Horizons in Cancer Therapies.* Springer; 2020. pp. 313–337.
15. Sakthi Devi R, Girigoswami A, Siddharth M, Girigoswami K. Applications of gold and silver nanoparticles in theranostics. *Applied Biochemistry and Biotechnology* 2022; 194(9): 4187–4219. doi: 10.1007/s12010-022-03963-z
16. Jagannathan NR. Potential of magnetic resonance (MR) methods in clinical cancer research. In: Sobti RC, Sobti A (editors). *Biomedical Translational Research*. Springer; 2022. pp. 339–360.
17. Haribabu V, Girigoswami K, Sharmiladevi P, Girigoswami A. Water—Nanomaterial interaction to escalate twin-mode magnetic resonance imaging. *ACS Biomaterials Science & Engineering* 2020; 6(8): 4377–4389. doi: 10.1021/acsbiomaterials.0c00409
18. Balasubramanian D, Girigoswami A, Girigoswami K. Antimicrobial, pesticidal and food preservative applications of lemongrass oil nanoemulsion: A mini-review. *Recent Advances in Food Nutrition & Agriculture* 2022; 13(1): 51–58. doi: 10.2174/2212798412666220527154707
19. Balasubramanian D, Girigoswami A, Girigoswami K. Nano resveratrol and its anticancer activity. *Current Applied Science and Technology* 2023; 23(3). doi: 10.55003/cast. 2022.03. 23.010
20. Metkar SK, Girigoswami K. Diagnostic biosensors in medicine—A review. *Biocatalysis and Agricultural Biotechnology* 2019; 17: 271–283. doi: 10.1016/j.bcab.2018.11.029
21. Ihtisham M, Noori A, Yadav S, et al. Silver nanoparticle's toxicological effects and phytoremediation. *Nanomaterials* 2021; 11(9): 2164. doi: 10.3390/nano11092164
22. Poonia K, Patial S, Raizada P, et al. Recent advances in Metal Organic Framework (MOF)-based hierarchical composites for water treatment by adsorptional photocatalysis: A review. *Environmental Research* 2023; 222: 115349. doi: 10.1016/j.envres.2023.115349
23. Keerthana V, Girigoswami A, Jothika S, et al. Synthesis, characterization and applications of GO-TiO_2 nanocomposites in textile dye remediation. *Iranian Journal of Science and Technology, Transactions A: Science* 2022; 46(4): 1149–1161. doi: 10.1007/s40995-022-01337-y
24. Vedhantham K, Girigoswami A, Harini A, Girigoswami K. Waste water remediation using nanotechnology—A review. *Biointerface Research in Applied Chemistry* 2021; 12(4): 4476–4495. doi: 10.33263/BRIAC124.44764495
25. Pallavi P, Harini K, Crowder S, et al. Rhodamine-conjugated anti-stokes gold nanoparticles with higher ROS quantum yield as theranostic probe to arrest cancer and MDR bacteria. *Applied Biochemistry and Biotechnology* 2023; 1–15. doi: 10.1007/s12010-023-04475-0
26. Deepika R, Girigoswami K, Murugesan R, Girigoswami A. Influence of divalent cation on morphology and drug delivery efficiency of mixed polymer nanoparticles. *Current Drug Delivery* 2018; 15(5): 652–657. doi: 10.2174/1567201814666170825160617
27. Piacentini E. Encapsulation efficiency. In: Drioli E, Giorno L (editors). *Encyclopedia of Membranes*. Springer; 2016. pp. 706–707.
28. Nishakavya S, Girigoswami A, Deepa R, et al. Size attenuated copper doped zirconia nanoparticles enhances in vitro antimicrobial properties. *Applied Biochemistry and Biotechnology* 2022; 194(8): 3435–3452. doi: 10.21203/rs.3.rs-807437/v1
29. Gowtham P, Girigoswami K, Pallavi P, et al. Alginate-derivative encapsulated carbon coated manganese-ferrite nanodots for multimodal medical imaging. *Pharmaceutics* 2022; 14(12): 2550. doi: 10.3390/pharmaceutics14122550
30. Drabczyk A, Kudłacik-Kramarczyk S, Głąb M, et al. Physicochemical investigations of chitosan-based hydrogels containing Aloe Vera designed for biomedical use. *Materials* 2020; 13(14): 3073. doi: 10.3390/ma13143073
31. Queiroz MF, Teodosio Melo KR, Sabry DA, et al. Does the use of chitosan contribute to oxalate kidney stone formation?. *Marine Drugs* 2014; 13(1): 141–158. doi: 10.3390/md13010141
32. Nagpal M, Singh SK, Mishra D. Superporous hybrid hydrogels based on polyacrylamide and chitosan: Characterization and in vitro drug release. *International Journal of Pharmaceutical Investigation* 2013; 3(2): 88–94. doi: 10.4103/2230-973X.114906

33. Jamnongkan T, Kaewpirom S. Potassium release kinetics and water retention of controlled-release fertilizers based on chitosan hydrogels. *Journal of Polymers and the Environment* 2010; 18: 413–421. doi: 10.1007/s10924-010-0228-6
34. Taha MO, Aiedeh KM, Al-Hiari Y, Al-Khatib H. Synthesis of zinc-crosslinked thiolated alginic acid beads and their in vitro evaluation as potential enteric delivery system with folic acid as model drug. *Die Pharmazie-An International Journal of Pharmaceutical Sciences* 2005; 60(10): 736–742.
35. Pereira R, Tojeira A, Vaz DC, et al. Preparation and characterization of films based on alginate and aloe vera. *International Journal of Polymer Analysis and Characterization* 2011; 16(7): 449–464. doi: 10.1080/1023666X.2011.599923
36. Han J, Zhou Z, Yin R, et al. Alginate–chitosan/hydroxyapatite polyelectrolyte complex porous scaffolds: Preparation and characterization. *International Journal of Biological Macromolecules* 2010; 46(2): 199–205. doi: 10.1016/j.ijbiomac.2009.11.004
37. Yuvarani I, Kumar SS, Venkatesan J, et al. Preparation and characterization of curcumin coated chitosan-alginate blend for wound dressing application. *Journal of Biomaterials and Tissue Engineering* 2012; 2(1): 54–60. doi: 10.1166/jbt.2012.1037
38. Liu S, Wang X, Pang S, et al. Fluorescence detection of adenosine-5'-triphosphate and alkaline phosphatase based on the generation of CdS quantum dots. *Analytica Chimica Acta* 2014; 827: 103–110. doi: 10.1016/j.aca.2014.04.027
39. Cai J, Chen X, Wang X, et al. High-water-absorbing calcium alginate fibrous scaffold fabricated by microfluidic spinning for use in chronic wound dressings. *Royal Society of Chemistry Advances* 2018; 8(69): 39463–39469. doi: 10.1039/C8RA06922K
40. Mello PA, Filippi-Chiela EC, Nascimento J, et al. Adenosine uptake is the major effector of extracellular ATP toxicity in human cervical cancer cells. *Molecular Biology of The Cell* 2014; 25(19): 2905–2918. doi: 10.1091/mbc.E14-01-0042
41. Li S, Li X, Guo H, et al. Intracellular ATP concentration contributes to the cytotoxic and cytoprotective effects of adenosine. *PLoS One* 2013; 8(10): e76731. doi: 10.1371/journal.pone.0076731
42. Schrader J. Ectonucleotidases as bridge between the ATP and adenosine world: Reflections on Geoffrey Burnstock. *Purinergic Signalling* 2022; 18(2): 193–198. doi: 10.1007/s11302-022-09862-6
43. Beldi G, Enjyoji K, Wu Y, et al. The role of purinergic signaling in the liver and in transplantation: Effects of extracellular nucleotides on hepatic graft vascular injury, rejection and metabolism. *Frontiers in Bioscience: A Journal and Virtual Library* 2008; 13: 2588–2603. doi: 10.2741/2868
44. Kukulski F, Lévesque SA, Sévigny J. Impact of ectoenzymes on p2 and p1 receptor signaling. *Advances in Pharmacology* 2011; 61: 263–299. doi: 10.1016/B978-0-12-385526-8.00009-6
45. Roberts V, Stagg J, Dwyer KM. The role of ectonucleotidases CD39 and CD73 and adenosine signaling in solid organ transplantation. *Frontiers in Immunology* 2014; 5: 64. doi: 10.3389/fimmu.2014.00064